ADVANCES IN ATMOSPHERIC SCIENCES, VOL. 23, NO. 3, 2006, 355–364

The Statistical Significance Test of Regional Climate Change Caused by Land Use and Land Cover Variation in West China

WANG Hanjie*[1] (王汉杰), SHI Weilai[2] (施伟来), and CHEN Xiaohong[3] (陈晓红)

[1] *Key Laboratory of Regional Climate-Environment Research for Temperate East Asia, Chinese Academy of Sciences, Beijing* 100029

[2] *Institute of Meteorology, PLA University of Science and Technology, Nanjing* 211101

[3] *Anhui Meteorological Observatory, Hefei* 230031

(Received 6 April 2005; revised 3 November 2005)

ABSTRACT

The West Development Policy being implemented in China is causing significant land use and land cover (LULC) changes in West China. With the up-to-date satellite database of the Global Land Cover Characteristics Database (GLCCD) that characterizes the lower boundary conditions, the regional climate model RIEMS-TEA is used to simulate possible impacts of the significant LULC variation. The model was run for five continuous three-month periods from 1 June to 1 September of 1993, 1994, 1995, 1996, and 1997, and the results of the five groups are examined by means of a student t-test to identify the statistical significance of regional climate variation. The main results are: (1) The regional climate is affected by the LULC variation because the equilibrium of water and heat transfer in the air-vegetation interface is changed. (2) The integrated impact of the LULC variation on regional climate is not only limited to West China where the LULC varies, but also to some areas in the model domain where the LULC does not vary at all. (3) The East Asian monsoon system and its vertical structure are adjusted by the large scale LULC variation in western China, where the consequences are the enhancement of the westward water vapor transfer from the east oast and the relevant increase of wet-hydrostatic energy in the middle-upper atmospheric layers. (4) The ecological engineering in West China affects significantly the regional climate in Northwest China, North China and the middle-lower reaches of the Yangtze River; there are obvious effects in South, Northeast, and Southwest China, but minor effects in Tibet.

Key words: West Development Policy of China, LULC variation, regional climate simulation, statistical t-test, East Asian monsoon

doi: 10.1007/s00376-006-0355-0

1. Introduction

There have been many studies on the possible impacts of land use and land cover (LULC) variation on regional climate. Chaney et al. (1977) studied the effect of desertification in the Sahara region on the local climate, showing that the precipitation decreased as the desert was enlarged; McGuffie et al. (1995) studied the global climate sensitivity to tropical deforestation; Lean and Rowntree (1997), and Gash and Nobre (1997) studied the effect of deforestation on the climate in the Amazon area, finding that if the forest was replaced by grassland, the surface temperature increased by 2.5°C and the annual evaporation and precipitation decreased by 30% and 25% respectively. Nicholson et al. (1998) studied the possible climate change in West Africa and its relationship with desertification, drought, and surface vegetation; Huang et al. (1995) studied the meteorological impact of replacing native perennial vegetation with annual agricultural species; which is nearly the opposite of the present study that replaces farmland with forest/grass.

In an over-populated developing country, the LULC varies more significantly in China than anywhere else around the world, so, Chinese scientists are paying special attention to the LULC variation. For instance, Liu and Wu (1997) studied the impacts of land surface on the onset of the summer monsoon, and

*E-mail: eerc2502@vip.sina.com

Zheng and Ni (1999) studied the effects of grassland desertification on summer drought in North China. A rather complete study is that of the work of Zheng et al. (2002a, 2002b), where within two continuous papers, the authors discussed both the simulation results and the possible mechanisms of the effects of vegetation change on the regional climate throughout China. These papers revealed the basic mechanism of regional climate change caused by the LULC variation and pointed out that severe vegetation degeneration would lead to a positive feedback between rainfall reduction and vegetation degradation. However, a less intensive degeneration might cause a negative feedback between deterioration and rainfall reduction. The results teach us to refrain from disturbing the natural ecosystems and to protect them from further deterioration. More recently, Wang et al. (2003) studied the regional climate effects of LULC variation in the last 300 years in China and pointed out that the conversion from forest to grass or crops that is related to deforestation and over-cultivation is the most dominant LULC variation in modern Chinese history. Regionally this conversion leads to significant warming over large areas of China and to the reduction of root zone soil moisture and latent heat fluxes. The change in temperature propagates to 1500 m above the surface and affects specific humidity throughout this part of the atmosphere. Wang and Zhou (2003) also studied the environmental effects of the world's largest afforestation engineering project, the 3N (Northeast, North and Northwest China) Shelter-belt Systematic Engineering Project in North China; as almost an opposite case to the previous deforestation activity, the construction of the 3N shelter belts could change the surface albedo, roughness length, as well as the heat and water vapor equilibrium parameters in the soil-vegetation-atmosphere interface and then the surface layer wind speed, temperature, humidity and precipitation. The consequences of the 3N shelter-belt construction are positive in improving the eco-environment in the northern parts of China, showing up as the reduction of surface wind speed, temperature and increased humidity, cloud cover, and precipitation.

The Chinese government started to pay special attention to environmental deterioration issues at the end of the 20th century. Sequentially, there have been three major ecological engineering projects in West China: the afforestation and/or natural forest protection engineering project, in the upper reaches of the Yangtze River and middle-upper reaches of the Yellow River, the desertification control engineering project in Northwest China, and the 4th construction engineering project of the 3N Shelter-belt Systematic Engineering Project following the previous three phases of the same project objectives.

In addition to the mass movement of replacing over-cultivated farmland with forest or grass and the virescence of the desertification land, the total forest (grass) coverage was increased significantly. Shi and Wang (2003) studied the regional climate effects of this latest LULC variation and concluded that the comprehensive effect of afforestation and the desertification land re-greening in West China would be beneficial to the eco-environment there. The pre-summer would be a little bit cooler and the rainfall during this period might be slightly increased. The simulation also showed that the large-scale LULC variation in Northwest China may have some effects on adjusting the structure of the East Asia Monsoon system and then the climate features in other parts of China.

Following Shi and Wang (2003), two different vegetation types are used for inter-comparison simulations: a real case and a virtual case. The former refers to the present LULC extracted from the Global Land Cover Characteristics Database (GLCCD) created by the U.S. Geological Survey (USGS) and the University of Nebraska-Lincoln (UNL) (Edinshink and Faundeen, 1994; Loveland and Belward, 1997), and the later represents the virtual case of land cover having been substantially changed due to the three major ecological engineering plans proposed by the Chinese government. In order to remove random errors of the individual case study, five continuous 3-month runs from 1 June to 1 September of 1993, 1994, 1995, 1996, 1997 are conducted by the same Regional Climate Model (RCM) configuration of Shi and Wang (2003). The model results are used for statistical significance analysis, which illustrate the difference of LULC variation impact around China and the actual effect of LULC variations rather than the random errors caused by individual case selection.

2. Model description and numerical simulation

The RCM used here is originally from the START Regional Center for Temperate East Asia (TEA), IAP (Institute of Atmospheric Physics), CAS (Chinese Academy of Sciences) and is called RIEMS-TEA (Regional Integrated Environmental Modeling System for Temperate East Asia) by Wei and Fu (1998) and Fu et al. (1999). Its thermodynamic frame is from the meso-scale model MM5 (Grell et al., 1994). It is a non-hydrostatic model and coupled to the surface model of Biosphere-Atmosphere Transfer Scheme (BATS) in order to study the air-vegetation interaction process. The RCM has a wide variety of available parameterizations for the land surface, the dynamics, and the radiation (Wei and Fu, 1998; Fu et al., 1999).

Based on the 1-km AVHRR (Advanced Very High Resolution Radiometer) NDVI (Normalized Difference

Vegetation Index) composites, the digital elevation data, the ecoregion interpretations, and the country- or regional-level vegetation and land use maps; the GLCCD is an accurate and up-to-date Geographic Information System (GIS) database for numerical modeling (Edinshink and Faundeen, 1994; Loveland and Belward, 1997). In order to feed the model, the overly-detailed vegetation types identified in the GLCCD are reclassified into 13 categories according to canopy similarity and seasonal phenological characteristics of different vegetation types (Wang et al., 2001). GLCCD also provides a convenient platform to describe any intentional LULC variation. For instance, during the ecological engineering planned in the West Development Policy, China is implementing an ecological engineering project called "stop farming and replace the farmland with forest/grass", with which about 24 million hectares of farmland will be replaced with either forest or grassland according to specific eco-environmental conditions, and such a large scale LULC variation cannot be ignored in the climate simulation. Another significant ecological engineering project is the 3N Shelter-belt Systematic Engineering project and re-greening the desertification lands. All of these can be handled by database operations as long as the planned area and the implementation locations are clarified; the LULC database operation can be done before any climate simulations take place.

Based on social investigation, we understand that in the first step of the plan, not all but only 25% of the present farmlands might be replaced with forest or grass, so the model is run for a virtual case in which 25% of the present farmland is replaced either with forest or with grassland. Whether the farmland is replaced with forest or with grassland depends on the cover fraction of vegetation type. If the forest covers a larger fraction than grassland within a numerical grid box, it implies that the eco-environmental conditions in this area are suitable for forest to grow; therefore, the farmland in this grid box is replaced with forest in the virtual case. Similarly, if the grassland covers a larger fraction than forest, the farmland is replaced with grassland. The forest or grass coverage is accounted for based on GLCCD's identification since the LULC resolution of the database is 1 km. Figure 1 illustrates the changed numerical grid boxes in from real vegetation to virtual vegetation in the model domain, and there are about 160 grid boxes in which the vegetation types are changed.

The RCM is capable of simulating the regional climate change caused by LULC variation because the key land surface parameters such as Leaf Area Index (LAI), albedo, roughness length, as well as various relevant thermodynamic properties of the LULC types are changed in the model. The LULC types are classified into 18–25 categories according to specific research interests, and the corresponding thermodynamic parameters are tabled frequently by modelers (Dickinson et al., 1993; Grell et al., 1994). Table 1 lists the parameters of the LULC types being changed in the virtual simulation study; it gives a better idea of how the model represents changes from farmland to grass or forest (Table 1).

The major limitation of the present model is the description of heterogeneous surface water balance processes in the air-vegetation-soil continuity. Compared with the atmospheric variables such as temperature or humidity, etc., the soil water or other vegetation parameters such as Leaf Area Index (LAI), stomatal conductance, etc., are more heterogeneous within a numerical grid box of 60 km×60 km, and the present RCM uses the average values of soil water content and other heterogeneous variables, which affects the accuracy of the output variables. As a matter of fact, such heterogeneity can be smoothed by a weighted average technique or corresponding mathematical operations since the satellite database provides very high-resolution LULC data, and the relevant model module is continually being improved. Of course, the prevailing model nesting technique is also an alternative way to reflect the surface heterogeneity; unfortunately, a nested simulation was not implemented because of limited computational facilities.

Table 1. The thermodynamic parameters that affect surface climate-environment in the climate simulation model.

LULC types	Max/min Leaf Area Index (LAI)	Albedo (%)	Roughness length (cm)	Minimum Stomatal resistance ($s\ m^{-1}$)	Moisture availability (%)	Thermal Inertia ($J\ cm^{-2}\ K^{-1}\ s^{-1/2}$)
Crop	6.0/0.5	18	15	120	30	0.17
Short grass	6.0/0.5	18	15	200	15	0.13
Tall grass	6.0/0.5	20	30	200	15	0.13
Evergreen forest	6.0/5.0	12	50	200	50	0.21
Deciduous forest	6.0/0.5	15	50	200	30	0.17
Desert	0.0/0.0	20	0.5	200	2	0.08

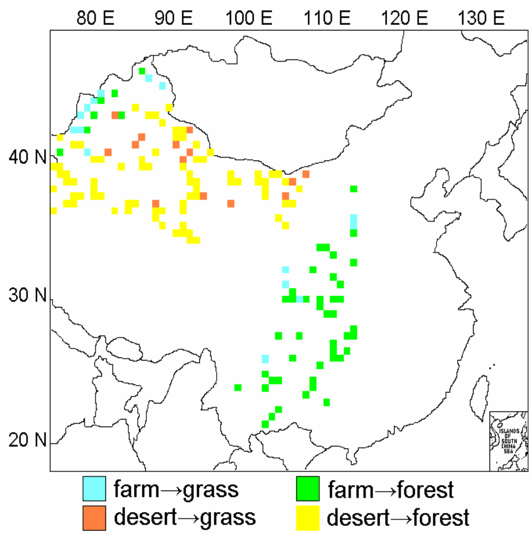

Fig. 1. The LULC-varied grid boxes within the model domain.

The model domain covers an area of 70 (in the east-west direction) ×60 (in the north-south direction) grid points, with each grid box being 60 km×60 km (Fig. 1). Vertically, the atmosphere is divided into 16 layers unequally according to the σ-coordinate system, where the sigma surface near the ground closely follows the terrain, and the higher-level sigma surfaces tend to approximate isobaric surfaces (Fu et al., 1999). In the present study, Anthes-Kuo's cumulus parameterization scheme (Anthes et al, 1984) and the CCM3 radiation parameterization scheme are selected. The model integration commences at 0000 LST 1 June and stops at 0000 LST 1 September of 1993, 1994, 1995, 1996, and 1997 with a time step of 120 seconds; so there are five groups for the sensitivity experiment, which satisfies the minimum requirement of student t-test statistics.

For convenience, the model outputs with respect to real vegetation cover are referred to as Model A and those with the virtual vegetation as Model B in the following sections; and the differences between Model A and Model B (Model B−Model A) are used to analyze the possible impacts of LULC variation.

3. Results and discussions

3.1 *Variation of the Climate variables and the statistical significance test*

Regional climate change is characterized by various climate variables, such as the surface temperature, relative humidity, wind strength as well as the periodic precipitation, etc. Figure 2a is the average daily ground temperature difference (Model B−Model A) over the integrated period from 1 June to 1 September. The shaded areas denote where the values of significance level are larger than 95%.

Figure 2a shows that the LULC variation causes ground temperature to decrease around China except in a few areas in Northeast China and North China. The lowest center is located in Northwest China where LULC is much more varied. The average value of temperature reduction is about -1°C and the lowest center has a value of -2.5°C. In general, LULC variation of the virtual vegetation leads to lower ground temperature, particularly in Northwest China, North China, and the middle-lower reaches of the Yangtze River. This means the LULC variation not only affects the climate in the western part of China, but also affects some other areas in the eastern part of China.

The statistical significance test shows (the shaded areas) that the LULC variation influences ground temperature significantly in most parts of Northwest China where LULC varies obviously, but there are also some areas in the eastern part of China, such as in North and Northeast China, the middle-lower reaches of the Yangtze and Huaihe Rivers etc.

Because of the ground temperature reduction, the upward longwave radiation from the surface is reduced after LULC variation. Figure 2b is the average daily upward longwave radiation in the integration period; the maximum value of the reduction is -25 W m^{-2} and is located in Northwest China. In the northern part of Sichuan Basin and the lower reaches of the Yangtze and Huaihe Rivers, there are two other negative value centers of longwave radiation, corresponding to the temperature reduction area shown in Fig. 2a. The land surface upward longwave radiation increases in the North China Plain and the Shandong Peninsula, which conflicts with the fact that ground temperature decreases (Fig. 2a) in this area. A possible explanation is that both humidity and precipitation in this area are increased (see Fig. 2c and Fig. 2d). The increased water vapor content means more cloud cover in the sky and larger amounts of upward longwave radiation reflection, which increases the ground temperature and then the upward longwave radiation.

The shaded areas in Fig. 2b show where the statistical significance level is greater than 95% by the student t-test for the upward longwave radiation. As compared to Fig. 2a, the confidence in Northwest China is similar, denoting that the longwave radiation changes as the ground temperature is reduced. On the other hand, the temperature is the only or dominant factor determining the longwave radiation in Northwest China. In the eastern part of China, however, the areas of high confidence level for long-wave radiation (Fig. 2b) are reduced significantly compared with those of ground temperature (Fig. 2a); the higher humidity and condensation cloud in this region might be the

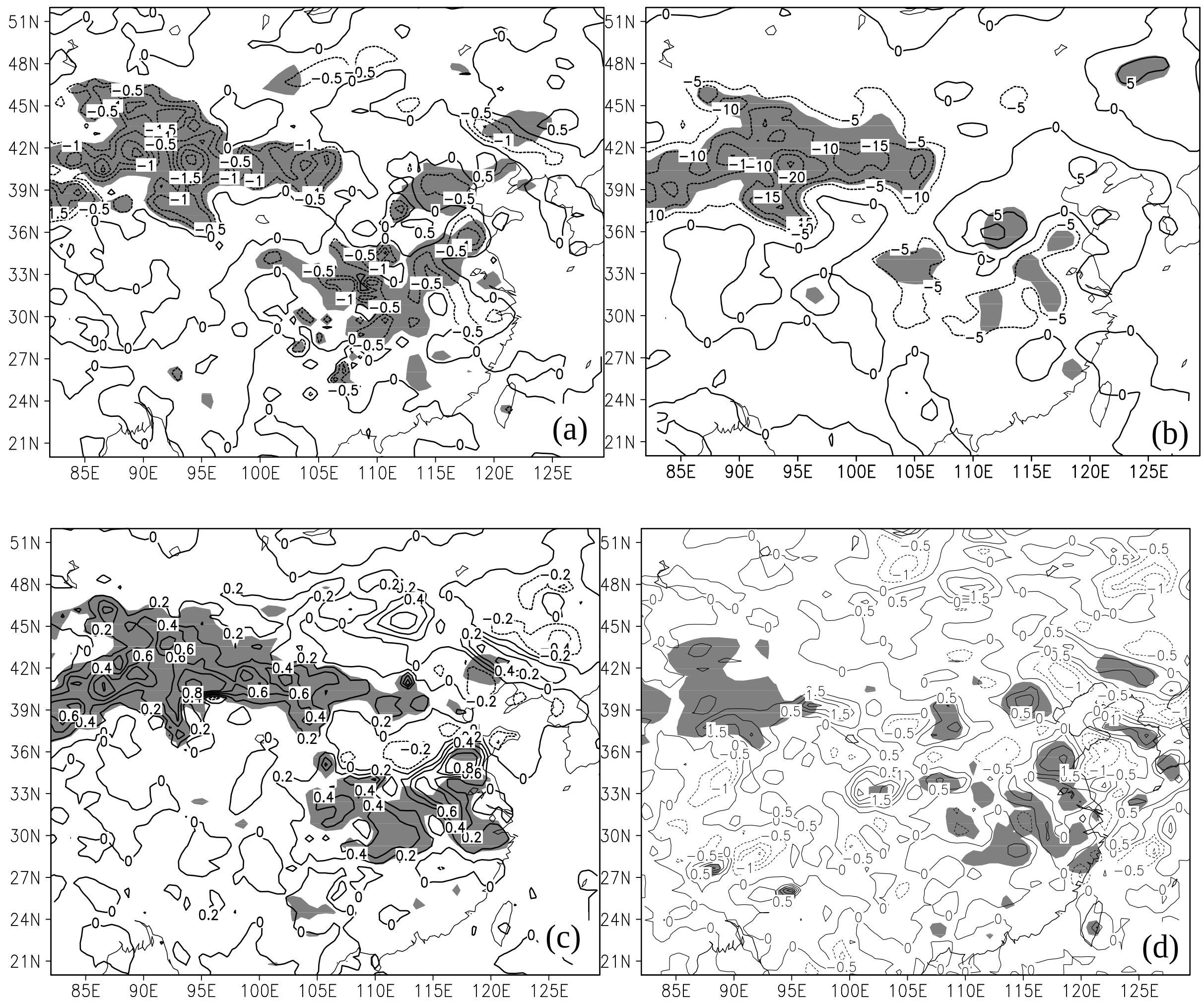

Fig. 2. The daily average difference between Model A and Model B (Model B−Model A) of (a) ground temperature (unit: °C), (b) upward longwave radiation (unit: W m^{-2}), (c) anemometer-high specific humidity (unit: g kg^{-1}), and (d) precipitation (unit: mm); the gray areas denote where the significance is larger than the 95% confidence level in the t-statistic test.

main reasons compensating for the reduction of upward longwave radiation. We prefer to conclude that the ground temperature is more sensitive to the LULC variation, while the longwave radiation can be affected by other factors such as cloud cover and air humidity in eastern China.

Figure 4 is the difference of specific humidity at the anemometer high before and after the LULC variation. The most significant area of humidity increase is in the northwest, the middle-lower reaches of the Yangtze and Huaihe Rivers, and the southern parts of North China, and the maximum value of increase is 1.0 g kg^{-1}. In some areas of Northeast China and North China, the humidity decreases slightly by a value of −0.2 to −0.4 g kg^{-1}. There is no significant influence in far Northeast and Southeast China, nor is there any in the Tibetan area.

The increased air humidity will increase the cloud cover and precipitation probability. Figure 2d shows the difference of rainfall between Model A and Model B. The precipitation increases over the continent of China except for a few areas on the China-Korea boundary, Yellow Sea, Southwest Tibet and Northeast China. In Northwest China, precipitation increases though the absolute value is small. In the east coast area, the positive and negative values are mixed, but on average, the positive values dominate the area.

From the statistical significance test (shaded area in Fig. 2d), the precipitation difference shows a high confidence level not only in Northwest China but also in East China as well, but there are more random uncertainties compared with Northwest China.

Following Shi and Wang (2003), the confidence level with respect to various climate factors in differ-

Table 2. The confidence level of the statistical t-test in different regions around China.

	Ground temperature	Anemometer-high specific humidity	Net upward longwave radiation	Precipitation
Northwest China	94%	96%	94%	88%
North China	93%	89%	89%	86%
Middle-lower reaches of the Yangtze River	90%	91%	88%	90%
Northeast China	87%	83%	85%	82%
Southwest China	85%	83%	80%	81%
South China	84%	84%	81%	83%
Tibetan Plateau	78%	79%	82%	74%

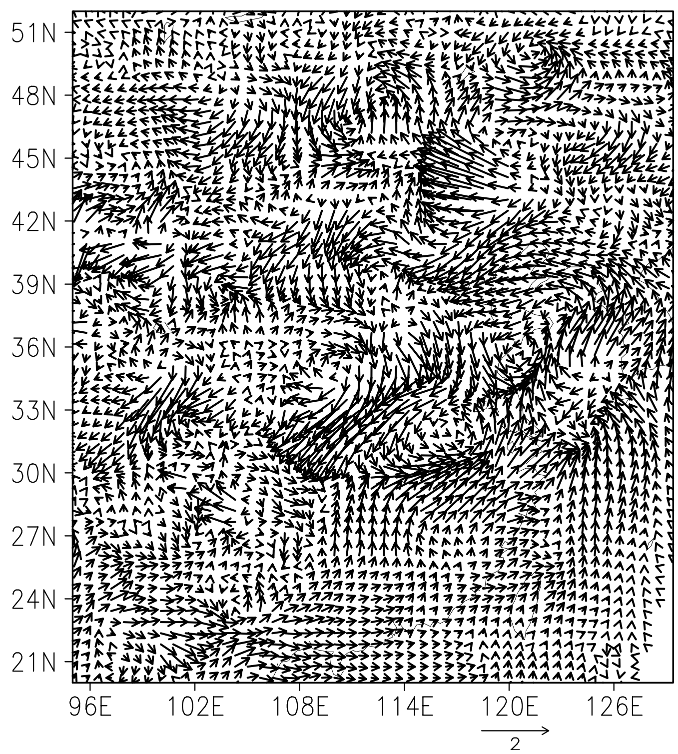

Fig. 3. The wind vector deviation between Model B and Model A at 850 hPa (units: m s^{-1}).

ent regions around China are listed in the Table 2 for comparison. The values listed in the table are averaged differences between Model A and Model B, and the climatic regions are classified according to the classical textbook *Physical Geography of China* (Zhao, 1984). Table 2 shows that the confidence level of the statistical t-test of the four climatic elements are greater than 85% in Northwest China, North China and the middle-lower reaches of the Yangtze River; between 80% and 85% in South China, Northeast China and Southwest China; except for the ground temperature in Northeast China. As for Tibet, the confidence levels of the four climatic variables are between 74% and 82%. The conclusion is that the LULC variation caused by the ecological engineering in West China significantly affects the regional climate in Northwest China, North China and the middle-lower reaches of the Yangtze River, and the climate in South China, Northeast China and Southwest China will be affected somehow as well, but the climate in the Tibetan Plateau is rarely disturbed.

3.2 *Mechanism analysis*

The prevailing studies have revealed the possible mechanism of the LULC variation affecting the regional climate (Wei and Fu, 1998; McGuffie et al., 1995; Zheng et al., 2002a, b; Wang et al., 2003). The explicit explanation is that the vegetated area has a smaller albedo, larger LAI and higher roughness length compared with desert or desertification land. As the bare soil is covered with more vegetation, the heat, water vapor and momentum equilibrium status in the surface layer will be changed, and the disequilibrium could be redistributed to an even larger extent by the atmospheric circulation governed by the thermodynamic equations of the climate model. The causality is simplified in Fig. 3, which shows that the consequence of vegetation cover increase is the reduction of surface temperature and the increase of possible precipitation.

A possible argument is raised about the surface temperature reduction after the vegetation cover increase. Since the albedo of the vegetated area is smaller than that of the desertification land (Table 1), the vegetated area receives more shortwave radiation; Shi and Wang (2003) showed that the daily-absorbed shortwave radiation can increase by 30 W s^{-2} under the same LULC change circumstances. Zheng et al. (2002b) found that shortwave radiation increased by 50 W s^{-2} under a virtual afforestation experiment in North China. So, the LULC variation dominated by replacing farmland and re-greening desertification lands with forest or grassland will eventually result in smaller albedo and more solar radiation absorption. It seems the surface temperature should be higher because of the increased shortwave radiation absorption, but the causality is not so simple. As a matter of fact, LULC variation not only changes the surface albedo but also the roughness length (Wang et al., 2001), which in turn causes the variation of surface wind profile and the turbulence structure, and then the variation of the heat and water vapor balance in the lower part of the atmosphere. Zheng et al. (2002a, b) argued that it is the increased soil water content in the vegetated area and the corresponding latent heat flux increase that causes the surface temperature reduction. The present simulation verified the conclusion by examining the model outputs of soil water content and latent heat flux (figures omitted). So, the surface temperature reduction is an integrated effect of the redistribution of momentum and heat and water vapor transfer in the land-vegetation-air continuity rather than the albedo alone, and so are the other regional climate variables.

3.3 *The adjustment of the East Asia Monsoon structure*

The East Asia Monsoon is one of the most important local atmospheric circulations caused by the thermal dynamic difference between land and sea (Ramage, 1971; Webster et al., 1998). It is expected that a significant LULC variation on the continent will adjust the monsoon circulation and its three dimensional structure. Liu and Wu (1997) pointed out the possible impacts of land surface changes on the onset of the East Asia Monsoon in summer; Fu (2004) studied the potential impacts of human-induced land cover change on the East Asia Monsoon; Shi and Wang (2003) pointed out that the large scale LULC variation in Western China might play some role in adjusting the East Asia monsoon and its vertical structure; their individual case study indicated that because of the same large-scale LULC variation, the south-secund wind has increased in the south and southwest parts of China, and the intensified southwest wind implies more water vapor transfer from the Indochina Peninsula and South China Sea. Besides, the wind field changed in the northern part of the eastern China coast, and the general feature is that the north-secund wind increases, and an additional east wind forms in the Shandong Peninsula and heads west to the central part of continental China; this benefits the westward water vapor transfer from the East Coast (Shi and Wang, 2003).

The present study shows similar characteristics. Figure 3 is the averaged wind vector difference at 850 hPa during the integration period. To the south of 30°N, the south-secund wind increased consistently, and the increased south wind meets the increased north wind and forms a shear line in the middle reaches of the Yangtze River. A strong, increased east wind appears in North-Northeast China, which is particularly beneficial to the water vapor transfer from the east coast to the central continent. In general, the figure shows a significant adjustment of lower level monsoon circulation.

In order to reveal the vertical structure of the monsoon circulation, sections are drawn of the averages of the differences between Model A and Model B in the latitude band 25°–45°N, which covers most parts of Mainland China and the area of LULC variation. The section is limited to the east of 95°E to keep away from the impact of the Tibetan Plateau. Figure 5a is the difference of vertical velocity due to the vegetation cover increase; the vertical velocity increases in the eastern part of China, which implies a thickened and enhanced East Asia Monsoon circulation. In the middle part of China (105°–116°E), the vertical velocity decreases though the absolute value is smaller, which can be attributed to the momentum conservation equation, and the subsided region corresponds to the humidity reduction (see the discussion of Fig. 5c below). Near the 105°E area, the vertical velocity increases again. To the west of 105°E, vertical velocity decreases, which might be caused by the boundary condition of the Tibetan Plateau.

Figure 5a also reveals the fact that the disturbance caused by the LULC variation penetrates into the whole layer of the atmosphere rather than being limited to the lower layers as we expected before. The

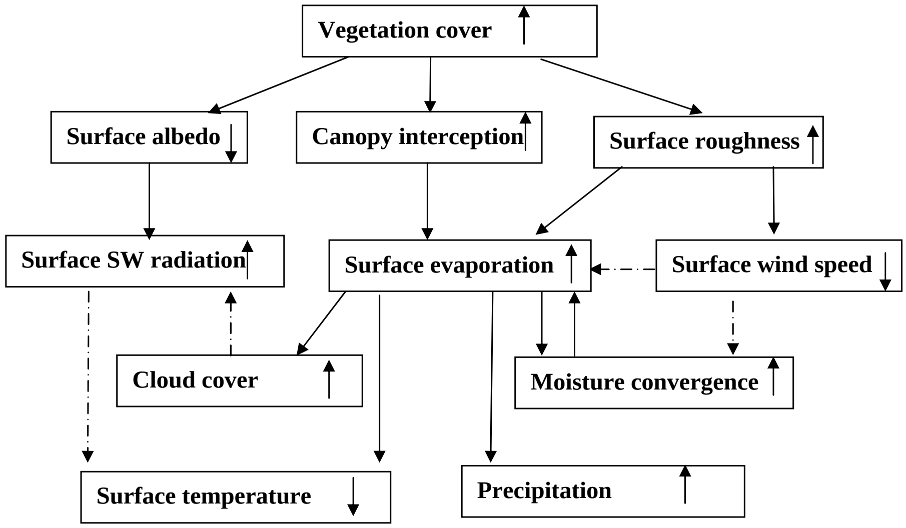

Fig. 4. The mechanism of vegetation cover increase affecting the regional climate, where SW is the abridged form of short wave, the arrows within the boxes show that the corresponding variable either increases (upward arrow) or decreases (downward arrow), and the arrows between each pair of text boxes denote either positive (solid arrow) or negative (dashed arrow) contributions from the original box variable to the destination one.

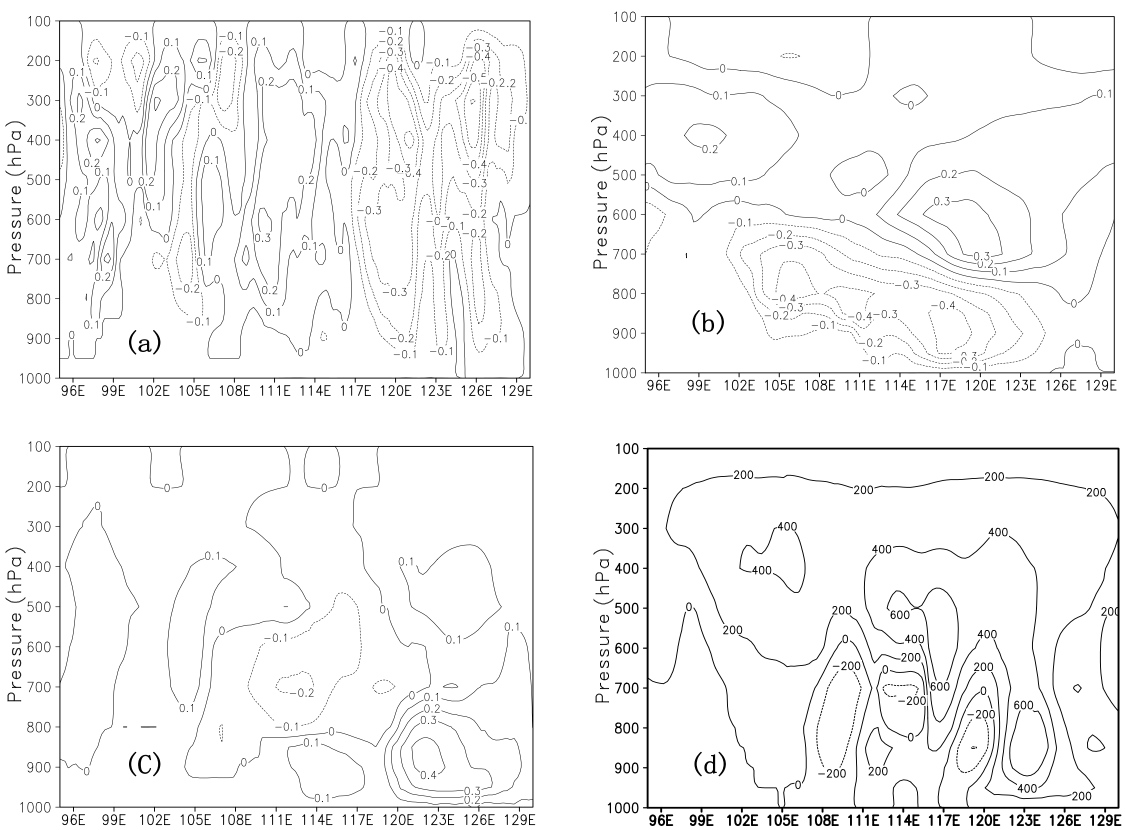

Fig. 5. West-East section of averaged difference between Model A and Model B (Model B−Model A) within the zone of 25°–45°N, (a) vertical velocity (unit: hPa s^{-1}), (b) temperature (unit: °C), (c) specific humidity (unit: g kg^{-1}), and (d) wet-hydrostatic energy (unit: J kg^{-1}).

published literature related LULC variation and its climate effect also reveals this fact as long as sections are used (Zheng et al., 2002a, b; Wang et al., 2003). Sections of temperature (Fig. 5b) and humidity (Fig. 5c) also show similar characteristics, but the differential values in the lower atmosphere are much larger than those in the upper parts of the atmosphere. Figure 5b shows that the temperature decreases in the lower parts of the atmosphere and increases in the upper parts. A separating layer that divides the negative and positive values declines from 600 hPa in the west to 800 hPa in the east coast area. The significant change reaches up to 300 hPa, and so does the specific humidity (Fig. 5c).

From the temperature variation, one expects a more stable atmospheric stratification, but the section of humidity shows that in the lower part of the atmosphere, the water vapor increases, particularly in the east coast area. The significant increase is limited to the lower level below 800 hPa, which should be attributed to the westward water transfer mentioned before. The middle layer humidity reduction in central China corresponds to the vertical velocity decrease shown in Fig. 5a.

What is the integrated consequence of the increased water vapor and stabilized atmosphere on regional precipitation? An effective variable called wet-hydrostatic energy that combines the effect of temperature and humidity is used to analyze the possible consequence on atmospheric stability and convective precipitation (Fig. 5d). The figure shows that after vegetation cover increases, wet-hydrostatic energy increases significantly in the middle-upper layers, and in the middle layer of central China, the wet-hydrostatic energy decreases slightly, which corresponds to the humidity reduction shown in Fig. 5c. But in general, wet-hydrostatic energy increases as the monsoon system is enhanced, and the highest level reaches up to 200 hPa. Zheng et al. (2002b) obtained similar results with their aforestation experiment in a rather smaller area of North China. The lager value of wet-hydrostatic energy means a more unstable atmosphere and more convective precipitation. This is consistent with the precipitation increase shown in Fig. 2d.

Unlike the prevailing studies on the relationship between LULC variation and regional climate change based on either a case of desertification or of an ecological restoration in a specific area (Liu and Wu, 1997; Wei and Fu, 1998; Zheng et al., 2002a, b), we have studied the most probable LULC variation around China based on the satellite-support database and the government-proposed West Development Policy and ecological restoration planning (see Fig. 1). The involved model grid boxes in which the LULC is varied in the climate model are scattered across western China except for the Tibetan Plateau. It is well known that the effect of LULC change on the regional climate depends mainly on the extent to which the LULC varies. The larger the scope of LULC variation, the more significant the regional climate change will be. The present paper assumes the largest extent of LULC variation and a rational change status according to governmental ecological construction planning; it reveals the important role of LULC variation on the East Asian Monsoon system and the relevant regional climate change.

4. Conclusions

The West Development Policy implemented in China has caused and will cause more significant LULC variation in West China. Based on high resolution LULC data extracted from the GLCCD, a regional climate model is run to reveal the possible regional climate changes across China. The main simulation results are:

(1) The regional climate is affected by the LULC variation because the equilibrium of water and heat transfer in the air-vegetation interface is changed. The ecological engineering implemented in West China will improve the eco-environment, showing as reduced temperature, increased humidity, and increased convective precipitation.

(2) The integrated impact of LULC variation on climate (such as temperature, humidity, net long wave radiation, and precipitation) is not only limited to West China, but also to the outside regions where the LULC does not vary.

(3) A statistical significance test reveals that the ecological construction in West China significantly affects the regional climate in Northwest China, North China and the middle-lower reaches of the Yangtze River; there are obvious influences in South, Northeast, and Southwest China, but little influence in Tibet.

(4) The structure and intensity of the East Asia summer monsoon system can be adjusted by the significant LULC variation around continental China, and the consequence of the vegetation cover increase is characterized by increased westward water vapor transfer, vertical velocity, wet-hydrostatic energy as well as convective precipitation.

Acknowledgments. This study was supported by the National Basic Research Program of China (Grant No. 2006CB400505), the Innovation Program of the Chinese Academy of Sciences (Grant No. ZKCX2-SW-210) and the National Natural Science Foundation of China (NSFC) (Grant No. 90302015).

REFERENCES

Anthes, R. A., Y. Hsie, and Y.H. Kou, 1984: Description of the PENN State/NCAR Meso-scale Model version (MM4). NCAR Technical Note, NCAR/TN-128+STR, 66pp.

Charney, J. C., W. J. Quick, S. H. Chow, and J. Kornfield, 1977: A comparative study of the effects of albedo change on drought in semi-arid regions. *J. Atmos. Sci.*, **34**, 1366–1388.

Dickinson, R. E., A. Henderson-Sellers, and P. J. Kennedy, 1993: Biosphere-Atmosphere Transfer Scheme (BATS) Version1e as Coupled to NCAR Community Climate Model. NCAR Tech. Note TN-387+STR, 72pp.

Edinshink, J. C., and J. L. Faundeen, 1994: The 1 km AVHRR Global land data first stages in implementation. *Int. J. Remote Sens.*, **15**, 3443−3462.

Fu Congbin, Wei Helin, and Qian Yun, 1999: Documentation on a Regional Integrated Environmental System (RIEMS Version 1), TEACOM Report (Seventh), No.1, START Regional Center for Temperate East Asia, Beijing, China, 26pp.

Fu Congbin, 2004: Potential Impacts of human-induced land cover change on East Asia monsoon. *The Development and Application Study of the Regional Integrated Environmental Modeling System* (*RIEMS*), Fu Congbin and Su Bingkai, Eds., China Meteorological Press, Beijing, 40–52. (in Chinese)

Gash, J. H. C., and C. A. Nobre, 1997: Climatic effects of Amazonian deforestation: Some results from ABRACOS. *Bull. Amer. Meteor. Soc.*, **78**, 823–830.

Grell, G. A., J. Dudhia, and D. R. Stauffer, 1994: A description of the fifth-generation Penn State/ NCAR mesoscale model (MM5). NCAR Technical Note, NCAR/TN-398+STR, 117pp.

Huang, Xinmei, T. J. Lyons, and R. C. G. Smith, 1995: Meteorological impact of replacing native perennial vegetation with annual agricultural species. *Hydrological Processes*, **9**, 645–654.

Lean, J., and P. R. Rowntree, 1997: Understanding the sensitivity of a GCM simulation of Amazonian deforestation to the specification of vegetation and soil characteristics. *J. Climate*, **10**, 1216–1235.

Liu Hui, and Wu Guoxiong, 1997: Impacts of land surface on climate of July and onset of summer monsoon. *Adv. Atmos. Sci.*, **14**, 289–309.

Loveland, T. R., and A. S. Belward, 1997: The IGBP-DIS global 1 km land cover data set, DISCover: First results. *Int. J. Remote Sens.*, **18**, 3289–3295.

McGuffie, K., A. Henderson-Sellers, H. Zhang, T. B. Durbidge, and A. J. Pitman, 1995: Global climate sensitivity to tropical deforestation. *Global and Planetary Change*, **10**, 97–128.

Nicholson, S. E., C. J. Tucker, and M. B. Ba, 1998: Desertification, drought, and surface vegetation: An example from the West African Sahel. *Bull. Amer. Meteor. Soc.*, **79**, 815–829.

Ramage, C. S. 1971: *Monsoon Meteorology.* Academic Press, London, 160pp.

Shi Weilai, and Wang Hanjie, 2003: The regional climate effect of replacing farmland and greening the desertification lands with forests or grassland in West China. *Adv. Atmos. Sci.*, **20**, 45–54.

Wang Hanjie, Li Yifan and A.K. Lo, 2001: A meso-β scale simulation of the effects of boreal forest ecosystem on the lower atmosphere. *Acta Meteorologica Sinica*, **15**, 116–128.

Wang H. J., and H. Zhou, 2003: A simulation study on the eco-environmental effects of 3-N shelter belts in North China. *Global and Planetary Change*, **37**, 231–246.

Wang H. J., A. J. Pitman, M. Zhao, and R. Leemans, 2003: The impact of land-cover modification on the June meteorology of China since 1700, simulated using a regional climate model. *International Journal of Climatology*, **23**, 511–527.

Webster, P. J., V. O. Magana, and T. N. Palmer, 1998: Monsoon: Process, Predictability, and the Prospects for Prediction. *J. Geophys. Res.*, **103**, 14451–14510.

Wei, H. L., and C. B. Fu, 1998: Study of the sensitivity of a regional model in response to land cover change over northern China. *Hydrological Processes*, **12**, 2249–2265.

Zhao Ji, 1984: *Physical Geography of China*, China Advanced Education Press, Beijing, 413pp. (in Chinese)

Zheng Weizhong, and Ni Yunqi, 1999: A numerical experiment study for effects of the grassland desertification on summer drought in North China. *Adv. Atmos. Sci.*, **16**, 251–262

Zheng Yiqun, Qian Yongfu, Miao Manqian, Yu Ge, Kong Yushou, and Zhang Donghua, 2002a: The effects of vegetation change on regional climate I: Simulation Results. *Acta Meteorologica Sinica*, **60**, 1–16. (in Chinese)

Zheng Yiqun, Qian Yongfu, Miao Manqian, Yu Ge, Kong Yushou, and Zhang Donghua, 2002b: The effects of vegetation change on regional climate II: Mechanism. *Acta Meteorologica Sinica*, **60**, 17–30. (in Chinese)